

Thermodynamic considerations about the formation of alloys by mechanical alloying

J. C. de Lima, V. H. F. dos Santos, T. A. Grandi, P. C. T. D'Ajello, and A. Dmitriev

Departamento de Física, Universidade Federal de Santa Catarina Florianópolis, CEP 88040-900, Santa Catarina, Brazil

(Received 4 January 2000; revised manuscript received 30 May 2000)

The formation of nanocrystalline and amorphous phases and unstable and stable solid solutions by mechanical alloying is analyzed by considering the mixture of the interfacial components of the elements as an ideal solution. We used the Gibbs free energy and equilibrium volume equations together with the results obtained for the excess Gibbs free energy for the metals, in nanometric form, to calculate activation energies associated with diffusive processes responsible for grain growth, grain boundary migration, atomic migration, and nucleation of new phases. Results obtained from this thermodynamic approximation seem to be confirmed experimentally by the formation of nanocrystalline $\text{Fe}_{67}\text{Ge}_{33}$ and amorphous $\text{Co}_{67}\text{Ge}_{33}$ alloys by mechanical alloying in our laboratory.

I. INTRODUCTION

The advent of nanostructured materials has made it possible to imagine a wide range of new technologies. This is associated with the presence of atomic arrangements located at defect centers, such as grain boundaries and interphase boundaries, allowing one to produce solids with new atomic structures and physical properties.

From a structural point of view, nanostructured materials can be regarded as being made up of two components, one crystalline, with dimensions on the order of some nanometers, that preserves the structure of bulk crystal, and another interfacial, composed of defects centers. Recently, the authors of Ref. 1, using radial distribution function (RDF) analysis, investigated the effect of mechanical milling on polycrystalline nickel. A comparison between the structure factors of nickel milled for 1 and 15 h shows a reduction of about 47% in the intensities of the peaks and a slight shift of peak positions to smaller K after 15 h of milling. This reduction was attributed to the interfacial component, which contained about 47% of the total number of atoms.

RDF analysis is not useful to obtain information about the interfacial component, because the contribution of this component overlaps the background in the x-ray-diffraction spectra, and both are filtered in the Fourier transform procedure to obtain the RDF. However, the existence of a large fraction of this component will not significantly change the density of the material. So the gaslike model for this component proposed by Gleiter² seems to be inappropriate. This argument is supported by the investigations on nanometric copper and cobalt carried out by Stern *et al.*³ and Babanov *et al.*,⁴ respectively. Those workers reported coordination numbers and interatomic distances associated with the first neighbors in this component.

The manipulation of the interfacial component makes it possible to design materials with desired physical properties for specific applications. As an example, in our laboratory we recently developed a technique, called thermomechanical alloying, to produce binary alloys starting with one of the components in nanometric form.^{1,5} The process uses the energy stored, via mechanical milling, in both components, and the high diffusivity⁶ observed in the nanocrystalline materials, to accelerate the solid-state reaction, increasing the reaction rate for the formation of alloys.

Conventional techniques such as arc melting do not permit the production of nanostructured materials. However, the techniques that do produce these materials (sputtering, synthesis from the gaseous phase, etc.)⁷ are highly complex, and require expensive equipment. Since the discovery that the mechanical alloying (MA) technique allows the synthesis of amorphous and crystalline phases and solid solutions, several nanostructured alloys were synthesized.⁸⁻¹¹ This technique presents several advantages compared with those mentioned earlier: the equipment is inexpensive and the process relatively simple, permitting the production of powder in bulk form and facilitating the fabrication of massive pieces via consolidation.¹² Although the MA technique is relatively simple, the physical mechanisms involved are not yet fully understood. In order to make use of this technique in industrial applications, a better understanding of these physical mechanisms is desirable.

In this paper, we analyze the formation of nanocrystalline and amorphous phases, unstable and stable solid solutions, by the MA process, considering that the interfacial components of the elements present in a mixture upon milling can be described as an ideal solution. Thus we used the Gibbs free energy and equilibrium volume equations of an ideal solution to analyze the phase compositions that will possibly nucleate and grow during the MA process. In order to examine the validity of this thermodynamic approximation, we applied it to several nanocrystalline and amorphous phases and unstable and stable solid solutions. We describe the results for nanocrystalline $\text{Fe}_{67}\text{Ge}_{33}$ and amorphous $\text{Co}_{67}\text{Ge}_{33}$ alloys produced in our laboratory using the MA technique.

II. THERMODYNAMICS OF MECHANICAL ALLOYING

Several metal powders have been obtained in nanometric form though high-energy ball milling.¹³ These studies show that in the first stage of milling the main effect is a reduction of particle size. Further milling, in addition to breaking the particles into smaller crystallites down to nanometer size, also produces an interfacial component made of defect centers. Nanometer powders must thus be analyzed in terms of two components, one crystalline and another interfacial.

From the thermodynamic point of view, a nanometric

powder is in a metastable state whose Gibbs free energy is greater than that of the crystalline state. To promote a transition from a nanometric state to a crystalline state, an activation energy must be supplied. This activation energy, which can be obtained by annealing, will trigger the diffusive processes responsible by the control of grain growth and grain boundary migration.

Mechanical alloying has been used for almost two decades as an alternative technique to obtain nanocrystalline or amorphous alloys starting from blended crystalline elemental metal powders. In the first stage of milling, there is a fast reduction in particle size of the mixture components and, after a short period of milling, the powder particles are cold welded by the colliding balls, resulting in composite powder particles which show a layered microstructure with a preferred orientation. Further milling leads to ultrafine composite powder particles where solid-state reactions take place. X-ray analysis shows that these ultrafine composite powder particles are composed by crystallites with sizes of a few nanometers.¹⁴ The reduction of crystallite size to a few nanometers cannot be accomplished without creating an interfacial component in each constituent.

It is well known that atoms along the grain boundaries require less energy to break away from their neighbors. However, grain boundaries are not the only locations of more energetic atoms. The atoms close to point or line defects also need less energy to migrate. These locations become more important as the temperature is lowered. The formation of several alloys at room temperature using the ball milling technique has been reported in the literature. In fact, nanometric materials have a high density of interfaces ($\approx 10^{19} \text{ cm}^{-3}$),⁶ and the component atoms show a higher self-diffusivity than single crystals and polycrystals with the same chemical composition.⁷ This indicates that the interfacial components of nanometric elements, which are composed of grain boundaries and interphase boundaries, are important in MA processes. Based on these considerations we believe that the solid-state reaction in MA starts in the mixture of the interfacial components of the elements in the ultrafine composite powder. A nanocrystalline or amorphous phase will not nucleate and grow unless an activation energy is supplied. This energy comes mainly from the balls. However, we believe that other processes can contribute to the energy balance, as the following arguments seem to indicate: (1) During ball milling of nickel, even after the crystallite size has stabilized at 15 nm for 30 h of milling, the crystalline component continues to store energy, reaching a saturation value of about 120 J g^{-1} ($\approx 0.073 \text{ eV/at}$) after 120 h of milling.¹ (2) If part of the energy coming from the balls is used for defect annealing, the energy thus released is available for the reaction; in the next collision, new defects are created, generating a continuous cycle. (3) If a new phase is nucleated locally, the energy released in the phase transformation can be transferred to the rest of the system. Thus the contribution of these three processes (ball collisions, defect annealing, and nucleation of a new phase) are the necessary ingredients for the energetic balance which defines the driving force in the process of formation of alloys in the MA technique.

In order to study the thermodynamic properties of formation of nanocrystalline and amorphous phases and unstable

and stable solid solutions by the MA technique and the stability of nanometric metals, we will assume the following model (hereafter called the IS model—from “ideal solution”): the mixture of the interfacial components of the elements in the ultrafine composite powder will be treated as an ideal solution. Consequently, a criterion to define a local minimum in the Gibbs free-energy function becomes necessary; otherwise, the Gibbs free-energy function decreases continuously, and phase transitions are not possible. Although the mixture of the interfacial components of the elements is a solid system, for practice reasons we will assume a cutoff value for the entropy as being the same as for the sublimation of a gas (about $2.5 \times 10^{-22} \text{ J/at K}$). The use of this cutoff value in the IS model means the entropy of the ideal solution may be overestimated, but the general conclusions of this work are not changed, because this will lead only to a shift in values of the activation energies.

Some ideas used to develop the IS model were based on work reported by Fecht¹⁵ about the thermodynamic properties and the stability of grain boundaries in nanometric metals, which are obtained by inert-gas condensation and compaction technique or by high-energy cyclic deformation processes produced in a standard ball mill.

The IS model applied to an A - B ideal solution can be described by the expressions for the Gibbs free energy and equilibrium volume of an ideal solution in the following form:¹⁶

$$\Delta G^{\text{is}} = x_A \Delta G_A + x_B \Delta G_B - RT[x_A \ln(1/x_A) + x_B \ln(1/x_B)], \quad (1)$$

$$(\Delta V/V_0)^{\text{is}} = x_A (\Delta V/V_0)_A + x_B (\Delta V/V_0)_B, \quad (2)$$

where x_i is the molar fraction and $(\Delta V/V_0)_i$, and ΔG_i are the excess volume and excess Gibbs free energy for the stabilization of A and B elements, in nanometric form, calculated in accordance with Fecht's work.

In the IS model, the activation energy necessary to nucleate a nanocrystalline or amorphous phase can be estimated as follows: once the excess Gibbs free-energy curve [Eq. (1)] is calculated, we identify on this curve $(\Delta V/V_0)^{\text{is}}$ [Eq. (2)] and the corresponding value of ΔG . The activation energy is the difference between the maximum (point B) and minimum (point A) values of ΔG , as shown in Fig. 1. The value $(\Delta V/V_0)^{\text{is}} = 0.0$ corresponds to the crystalline state.

In the last two decades, a number of publications have appeared on the amorphization of alloy powders by the MA technique, but very few papers deal with the formation of intermetallic compounds and fewer still with the synthesis of supersaturated solid solutions. More recently, it was shown that solid solutions composed of immiscible elements (positive heat of mixing) can also be formed by ball milling. Several authors tried to describe the physical mechanisms leading to the formation of nanocrystalline or amorphous phases and stable and unstable solid solutions, but up to now a complete explanation is missing. Based on the assumptions that the mixture of the interfacial components of the elements can be described as an ideal solution and that the nucleation of the crystalline or amorphous phase starts at the ideal solution, we will try to analyze the formation of these phases as well as the formation of unstable and stable solid solutions in the MA technique.

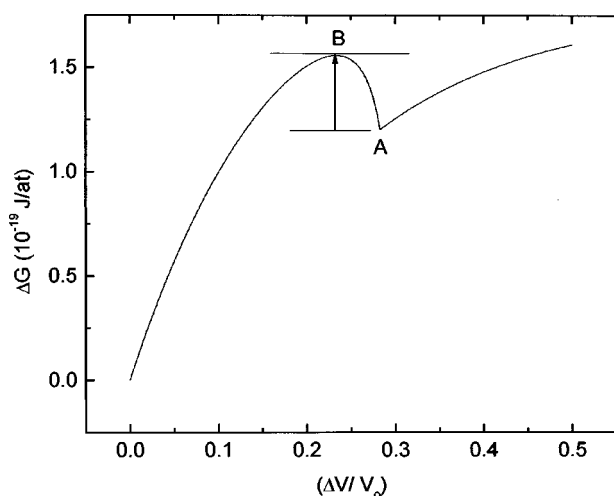


FIG. 1. Procedure to estimate the activation energy for an ideal solution from the excess Gibbs free energy as function of excess volume curve calculated at a specific temperature.

In recent years, we used the MA technique to produce and study the $\text{Fe}_{25}\text{Zn}_{75}$,¹⁷ $\text{Ni}_{20}\text{Zn}_{80}$,⁵ $\text{Cu}_{67}\text{Al}_{33}$,⁸ $\text{Cu}_{33}\text{Al}_{67}$, $\text{Fe}_{30}\text{Co}_{70}$, and $\text{Co}_{20}\text{Zn}_{80}$ nanocrystalline alloys, as well as some amorphous alloys such as FeAl_4 . In order to compare our theoretical results with a wider set of experimental data, we have taken from the literature some mixtures that resulted in the formation of $\text{Nb}_{75}\text{Ge}_{25}$,¹⁸ Ni_2Zr ,¹⁹ and $\text{Fe}_{50}\text{Zr}_{50}$ (Ref. 14) amorphous alloys. Also, we have considered solid solutions of Zn in Cd reported in the literature,¹⁰ as well as the formation of unstable solid solutions composed of immiscible elements such as Cu-Fe,²⁰ Cu-W,²¹ Cu-Ta,²² and Cu-V,²³ using the MA technique.

In our laboratory, milling of mixtures composed of metallic elements was performed using a fan to keep the temperature of the cylindrical steel vial containing the powders and steel balls below 323 K. In order to study the kinetics of the formation of phases in the systems above, we calculated the excess Gibbs free energy for each element, at temperatures of 300, 323, and 373 K, according to Fecht's work. Thus, for each of the systems above, it was possible to investigate the activation energies for several ideal solutions of the type A_xB_{1-x} , where $x = 10, 20, 30, 40, 50, 60, 70, 80,$ and 90 and, using Eqs. (1) and (2), to determine the excess Gibbs free energy and the excess equilibrium volume. Considering the systems for which we have obtained the formation of the nanocrystalline alloys, the ideal solutions that show smaller activation energy are those with compositions close to that of the alloys $\text{Fe}_{25}\text{Zn}_{75}$, $\text{Ni}_{20}\text{Zr}_{80}$, $\text{Cu}_{67}\text{Al}_{33}$, $\text{Cu}_{33}\text{Al}_{67}$, $\text{Fe}_{30}\text{Co}_{70}$, and $\text{Co}_{20}\text{Zn}_{80}$. For these ideal solutions, the calculated activation energy values, at the three temperatures above, are between 0.030 and 0.080 eV/at. For the systems Nb-Ge, Ni-Zr, and Fe-Zr which resulted in amorphous alloys, the ideal solutions showing smaller activation energy are those with compositions close to that of the amorphous alloys $\text{Nb}_{75}\text{Ge}_{25}$, Ni_2Zr , and $\text{Fe}_{50}\text{Zr}_{50}$. For these ideal solutions, the calculated activation energy are smaller than 0.030 eV/at. For other compositions, we found an activation energy that can reach up to 0.110 eV/at. For the stable solid solutions of Zn in Cd investigated in Ref. 10, the compositions of ideal solutions showing smaller activation energies are those reported by the authors, i.e., between 20 and 60-at% Zn. For

these ideal solutions, the calculated activation energy is about 0.150 eV/at. For almost all the systems mentioned above, formed by immiscible elements, the ideal solutions have an activation energy close to zero, similar to the ones found for the amorphous alloys. Among the systems investigated, only the Fe-Cu system has relatively large activation energies, between 0.070 and 0.110 eV/at, for any composition of the ideal solution.

To understand the formation of these alloys, knowledge of other physical mechanisms is necessary in addition to two key considerations pertinent to the formation of amorphous and crystalline alloys: (i) the two elements must have a large negative relative heat of mixing, and (ii) either one of them must be an anomalously fast diffuser (to produce an amorphous phase). In addition, the two elements must have similar diffusion coefficients, as the formation of the crystalline phase requires the simultaneous diffusion of the components.²⁴

We believe that the three processes responsible for the driving force, already discussed, play an important role in the formation of nanocrystalline alloys by the MA process. We also believe that because the temperatures reached during milling are very low, most of the energy available is used to trigger the mechanisms whose activation energies are between 0.030 and 0.070 eV/at. However, this energy is not enough to eliminate the initial ideal solutions completely, resulting in a final nanocrystallized alloy which still contains part of these ideal solutions which will form its interfacial component. This seems to be supported by following arguments: (i) most of the nanocrystalline alloys obtained are poorly crystallized, in spite of the high density of interfaces and the enhanced diffusivity coefficients observed in nanometric materials; and (ii) in some cases, when the final product is annealed, new phases are formed and/or one or more elements segregate.

With respect to the formation of amorphous alloys using the MA process, we believe that, beyond the large negative relative heat of mixing, only a small fraction of the total available energy is expended to activate those mechanisms whose activation energies are smaller than 0.030 eV/at. Thus, considering the high density of interfaces and the enhanced diffusivity coefficients observed in nanometric materials, the energy balance is enough to promote the diffusion of the atomic species. Besides this fact, if one of them has a very high mobility, being a fast diffuser when compared with the other, the stoichiometry necessary for the formation of the crystalline phase will probably not be reached. Thus the most probable outcome is an amorphous structure.

Based in ideal solutions investigated in the Zn-Cd system, we think that, in spite of the small negative relative heat of mixing, the total available energy during milling is not enough to activate those mechanisms whose activation energies are about 0.150 eV/at. Thus there is no solid-state reaction, and the available energy is used to dissolve an atomic species into the lattice of the other.

As to the formation of the unstable solid solutions composed of immiscible elements using the MA technique, we believe that in spite of the positive heat of the mixture, since the activation energies are very small, the energy coming from the balls and the annealing of defects is enough to promote diffusion, resulting in an unstable solid solution. Subsequent annealing promotes the dissociation of the elements.¹¹

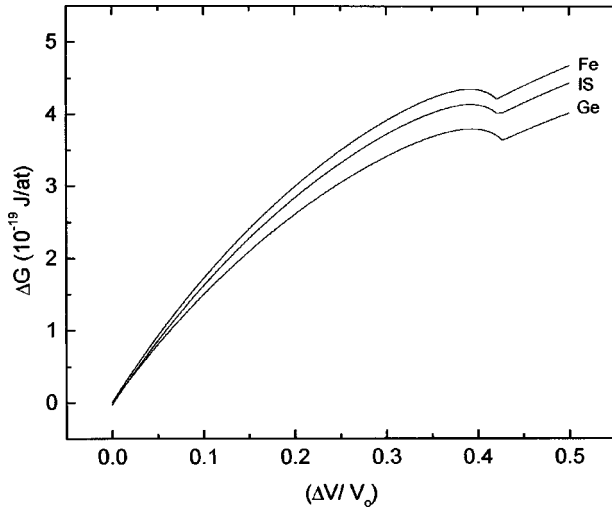


FIG. 2. The excess Gibbs free energy as function of excess volume curve for the $\text{Fe}_{67}\text{Ge}_{33}$ ideal solution (middle), calculated at 323 K. We also show the excess Gibbs free energy as a function of excess volume curves for the Fe and Ge, in the nanometric form, calculated in according to Fecht's work (Ref. 15).

III. EXPERIMENTAL PROCEDURE

Mixtures of commercial iron, cobalt, and germanium (purity > 99.5%) with nominal compositions $\text{Fe}_{67}\text{Ge}_{33}$ and $\text{Co}_{67}\text{Ge}_{33}$ were prepared and milled for 28 and 29 h, respectively, under an argon atmosphere in a Spex 8000 shaker mill, using spheres and a cylindrical steel vial. We used five balls with a diameter of 10 mm, giving a weight ratio to powder of 5:1. A fan was used to keep the temperature near room temperature. The milled powder samples were analyzed, via x-ray diffraction, with a Siemens diffractometer using $\text{Co } K\alpha$ radiation ($\lambda = 0.179\,026$ nm).

IV. APPLICATION OF THERMODYNAMIC CONSIDERATIONS IN THE PREPARATION OF $\text{Fe}_{67}\text{Ge}_{33}$ AND $\text{Co}_{67}\text{Ge}_{33}$ ALLOYS

A. Nanocrystalline $\text{Fe}_{67}\text{Ge}_{33}$ alloy

Figure 2 shows the excess Gibbs free energy (middle) at 323 K for the $\text{Fe}_{67}\text{Ge}_{33}$ ideal solution, calculated using Eq. (1) with the excess Gibbs free-energy curves calculated at

the same temperature for Fe and Ge in nanometric form. In this figure, $\Delta V/V_0 = 0.0$ corresponds to the crystalline state. The Gibbs free-energy curves for Fe and Ge show local minima at $(\Delta V/V_0)_{\text{Fe}} = 0.421$ and $(\Delta V/V_0)_{\text{Ge}} = 0.428$. At this temperature, for a nanometric-crystalline phase transition to occur, the Fe and Ge atoms located at the interfacial components need an activation energy of 1.35×10^{-20} J/at (≈ 0.084 eV/at) and 1.54×10^{-20} J/at (≈ 0.096 eV/at), respectively. Yet, according to Fig. 2, the ideal solution has an excess volume, calculated using Eq. (2), close to those elements.

Table I shows the theoretical values of the activation energy and excess volume for different ideal solutions of Fe and Ge at 300, 323, and 373 K. According to this table, the ideal solutions with smaller activation energies are those with compositions between 50-at. % Fe (1.17×10^{-20} J/at or ≈ 0.073 eV/at) and 70-at. % Fe (1.18×10^{-20} J/at or ≈ 0.074 eV/at). Thus, based on this table, we chose a mixture of commercial iron and germanium with a nominal composition $\text{Fe}_{67}\text{Ge}_{33}$ to investigate the possibility of forming this alloy by the MA technique.

After 28 h of milling, the mixture had become a very fine black powder; its x-ray-diffraction pattern (XRD), displayed in Fig. 3 (curve A), showed a stable phase quite different from those of the pure Fe and Ge. The broad peaks are suggestive of a product with very small crystallite size as well as poor crystallinity, as expected. Applying the Scherrer formula²⁵ to the highest peak, we obtained a mean crystallite size of about 6 nm.

According to the Joint Committee on Powder Diffraction Standards cards, the phases nucleated in the composition range explored in our experiments could be any of the following: FeGe (hcp), $\text{Fe}_{1.4}\text{Ge}$ (hcp), $\beta\text{-Fe}_{1.6}\text{Ge}$ (hcp), $\text{Fe}_{1.5}\text{Ge}$ (orthorhombic), $\text{Fe}_{3.36}\text{Ge}_{1.97}$ (hcp), Fe_6Ge_5 (monoclinic), $\text{Fe}_{0.565}\text{Ge}_{0.435}$ (hcp) and $\text{Fe}_{0.615}\text{Ge}_{0.385}$ (hcp). Since many of the ideal solutions have similar activation energies (see Table I), it is also possible that more than one phase could be nucleated simultaneously. In order to identify the nucleated phase corresponding to the XRD pattern displayed in Fig. 3 (curve A), each alloy was simulated using the Rietveld²⁶ structure refinement method together with the atomic coordinates and temperature factors given in Refs. 27 and 28. The best fitting was obtained considering the data for the Fe_5Ge_3 and FeGe alloys and the simulated XRD patterns are

TABLE I. Theoretical values of the activation energy (E_a) and excess volume ($\Delta V^{\text{IS}} = \Delta V/V_0$) for different ideal solutions of Fe and Ge at 300, 323, and 373 K.

Fe (at. %)	ΔV^{IS}	300 K		323 K		373 K	
		E_a 10^{-19} J/at	E_a (eV)	E_a 10^{-19} J/at	E_a (eV)	E_a 10^{-19} J/at	E_a (eV)
10	0.427	0.1231	0.077	0.1473	0.092	0.2038	0.127
20	0.427	0.1176	0.073	0.1416	0.088	0.1979	0.123
30	0.426	0.1121	0.070	0.1295	0.081	0.1836	0.114
40	0.425	0.1066	0.066	0.1216	0.076	0.1740	0.109
50	0.424	0.1011	0.063	0.1175	0.073	0.1689	0.105
60	0.424	0.0956	0.060	0.1172	0.073	0.1691	0.105
70	0.423	0.1005	0.063	0.1184	0.074	0.1701	0.106
80	0.422	0.1044	0.065	0.1231	0.077	0.1751	0.109
90	0.422	0.1082	0.068	0.1261	0.079	0.1790	0.112

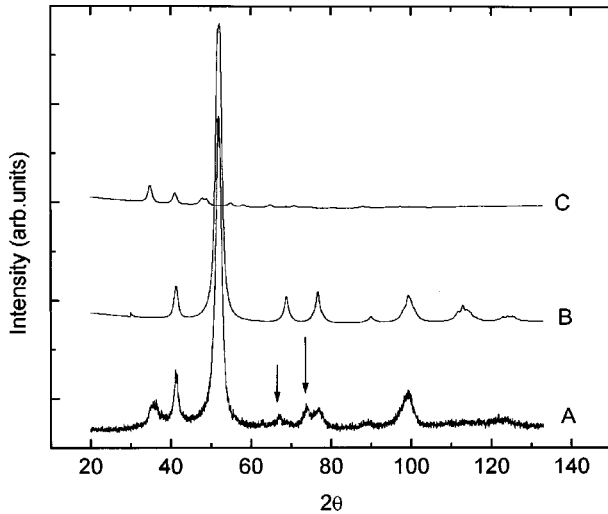


FIG. 3. Experimental and simulated x-ray-diffraction patterns: for the as-milled $\text{Fe}_{67}\text{Ge}_{33}$ alloy (A), simulated for the Fe_5Ge_3 alloy (B) and simulated for the FeGe alloy (C).

shown in Fig. 3 (curve B for the Fe_5Ge_3 alloy and curve C for the FeGe alloy). The ratio of scale factors used for the simulation of these two phases is approximately 18, indicating that the volume fraction of the Fe_5Ge_3 phase is greater than the one for the FeGe phase. There are two peaks in curve A (indicated by an arrow) which do not belong to any of these phases. Probably, they are related with a third phase which we could not identify.

It is interesting to observe that at 373 K the activation energies shown on Table I are greater than 0.100 eV/at. According to our thermodynamic considerations, these values are as high as those found for the formation of the stable solid solutions. This fact reinforces the idea that the new structures formed by the MA technique are associated with the energy balance involving the magnitude of the heat of mixing and the energy necessary to activate migration defects. This means that the theoretical energy activation is a good parameter to predict the nucleated phases, but it is also necessary to take into account the other aspects mentioned early. As an example, Fig. 3 shows that after 28 h of milling the final product is a nanocrystalline alloy and not a solid

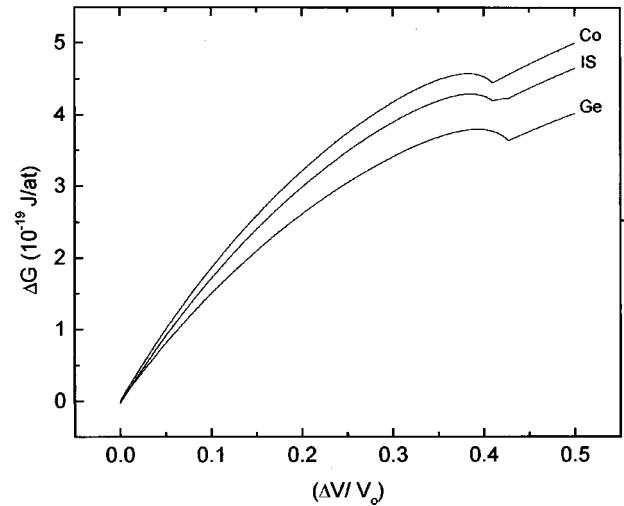


FIG. 4. The excess Gibbs free energy as function of excess volume curve for the $\text{Co}_{67}\text{Ge}_{33}$ ideal solution (middle), calculated at 323 K. Also shown is the excess Gibbs free energy as a function of excess volume curves for Co and Ge, in the nanometric form, calculated in according to Fecht's work (Ref. 15).

solution. This is taken as evidence that the total energy available during milling is sufficient to nucleate new phases and promote annealing defects.

B. Amorphous $\text{Co}_{67}\text{Ge}_{33}$ alloy

The same thermodynamic considerations used to study the Fe-Ge system and described in Sec. IV A were used to investigate the Co-Ge system. Figure 4 shows the excess Gibbs free energy curve (middle), calculated at 323 K, for the $\text{Co}_{67}\text{Ge}_{33}$ ideal solution using the excess Gibbs free-energy curves, calculated at the same temperature, for the elements Co and Ge in nanometric form. The excess Gibbs free-energy curves for the nanometric elements Co and Ge show local minima at $(\Delta V/V_0)_{\text{Co}} = 0.410$ and $(\Delta V/V_0)_{\text{Ge}} = 0.428$. At this temperature, for a nanometric-crystalline phase transition to occur, the Co and Ge atoms located at the interfacial components need activation energies of 1.28×10^{-20} J/at (≈ 0.080 eV/at) and 1.54×10^{-20} J/at (≈ 0.096 eV/at), respectively.

TABLE II. Theoretical values of the activation energy (E_a) and excess volume ($\Delta V^{\text{IS}} = \Delta V/V_0$) for different ideal solutions of Co and Ge at 300, 323, and 373 K.

Co (at. %)	ΔV^{IS}	300 K		323 K		373 K	
		E_a 10^{-19} J/at	E_a (eV)	E_a 10^{-19} J/at	E_a (eV)	E_a 10^{-19} J/at	E_a (eV)
10	0.426	0.1045	0.065	0.1277	0.080	0.1818	0.113
20	0.424	0.0788	0.049	0.1001	0.062	0.1500	0.094
30	0.423	0.0655	0.041	0.0862	0.054	0.1349	0.084
40	0.421	0.0541	0.034	0.0738	0.046	0.1204	0.075
50	0.419	0.0499	0.031	0.0690	0.043	0.1146	0.071
60	0.417	0.0521	0.032	0.0712	0.044	0.1166	0.073
70	0.415	0.0602	0.038	0.0796	0.050	0.1257	0.078
80	0.414	0.0689	0.043	0.0891	0.056	0.1371	0.086
90	0.412	0.0859	0.054	0.1071	0.067	0.1571	0.098

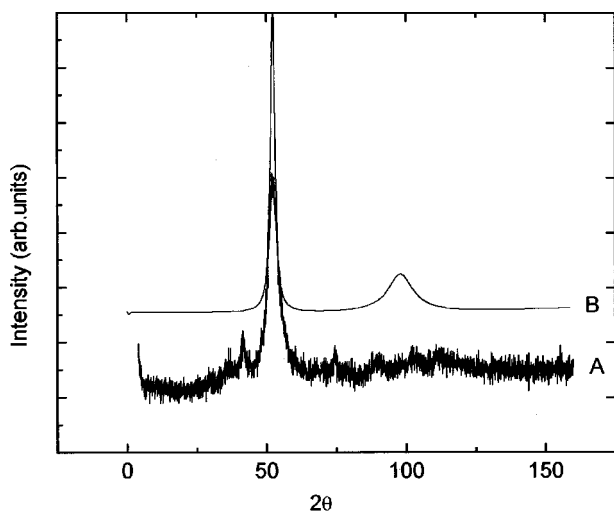


FIG. 5. Experimental and simulated x-ray-diffraction patterns for the as-milled $\text{Co}_{67}\text{Ge}_{33}$: measured after 29 h of milling (A) and simulated using the random hard-sphere packing model (B).

Table II shows the activation energies and excess volumes for different ideal solutions of Co and Ge at 300, 323, and 373 K. According to this table, the ideal solutions showing smaller activation energies are those with compositions between 40-at. % Co (0.73×10^{-20} J/at or ≈ 0.046 eV/at) and 70-at. % Co (0.79×10^{-20} J/at or ≈ 0.049 eV/at). It was seen early that the mixtures which produced amorphous alloys by the MA process had activation energy of ≈ 0.030 eV/at or smaller. Considering that the energy associated with the balls plus the energy from annealing of defects is greater than 0.030 eV/at, we believe that amorphous $\text{Co}_x\text{Ge}_{1-x}$ alloys with compositions in the interval above could be produced by the MA technique. In order to verify this assumption, we chose a mixture of commercial cobalt and germanium with nominal composition $\text{Co}_{67}\text{Ge}_{33}$. This composition was chosen because in the literature there is an investigation about the amorphization of the intermetallic compounds $\alpha\text{-Co}_2\text{Ge}$ and $\beta\text{-Co}_2\text{Ge}$ upon mechanical milling carried out by Zhou and Bakker.²⁹ Thus it was possible to compare our XRD data directly with those reported by these authors.

After 29 h of milling, the mixture was a very fine black powder; its x-ray-diffraction pattern is displayed in Fig. 5 (curve A). The absence of the well-defined peaks above $2\theta = 50^\circ$ and the presence of a large and strong diffuse halos at about $2\theta = 50^\circ$ characterizes the XRD pattern of an amorphous phase. The presence of some sharp peaks associated with pure elements shows that the amorphous alloy is not completely formed for this milling time. A comparison of this XRD pattern with the ones reported by Zhou and Bakker²⁹ for orthorhombic $\alpha\text{-Co}_2\text{Ge}$ (low-temperature phase) shows that our data are comprised between their data

measured for 40 and 60 h of milling. This indicates that by increasing milling time a homogenous amorphous phase could be obtained. In addition, the appearance of an amorphous phase is confirmed by the simulated XRD pattern (curve B) for the Co_2Ge amorphous phase using the random hard-sphere packing model. This result seems to support the assumption that decreasing the activation energies of the ideal solutions increases the probability of obtaining amorphous phases due to the fact that more energy is available to promote atomic diffusion. In addition, Table II shows that amorphous Co-Ge alloys with compositions around 50-at. % Co could be produced by the MA process.

V. CONCLUSIONS

Based on the results described earlier, we can conclude that the following.

(1) The formation of nanocrystalline and amorphous phases and unstable and stable solid solutions by mechanical alloying may be analyzed regarding the mixture of the interfacial components of the elements as an ideal solution. This seems to be confirmed by experimental results for the Fe-Ge and Co-Ge systems.

(2) In general, nucleation of nanocrystalline phases seems to occur when the activation energy is between 0.030 and 0.080 eV, while amorphous phases are nucleated for activation energy smaller than 0.030 eV.

(3) According to the results for the Zn-Cd system, stable solid solutions seem to occur when the activation energy is greater than 0.150 eV, while for unstable solid solutions formed by immiscible elements, the activation energy is much smaller, in the same range as for amorphous phases. Thus, in spite of the positive heat of mixing, unstable solid solutions are formed due to the high diffusivity coefficients associated with the MA process, combined with the three energetic processes described in the text.

(4) Use of the activation energy, estimated according to the IS model for the mixture of the interfacial components of the elements in the ultrafine composite powder, seems to be a good alternative method to design and predict the final products in MA experiments. However, knowledge of other physical mechanisms is necessary besides the two mechanisms related to the formation of amorphous and crystalline alloys which are described in this work.

ACKNOWLEDGMENTS

We thank the Conselho Nacional de Desenvolvimento Científico e Tecnológico—CNPq and the Agência Financiadora de Projectos—FINEP for material and financial support. We thank R. S. de Biasi for suggestions and for a careful reading of the manuscript.

¹T. A. Grandi, V. H. F. dos Santos, and J. C. De Lima, *Solid State Commun.* **112**, 359 (1999).

²H. Gleiter, *Nanostruct. Mater.* **1**, 1 (1992).

³E. A. Stern, R. W. Siegel, M. Newville, P. G. Sanders, and D. Haskel, *Phys. Rev. Lett.* **75**, 3874 (1995).

⁴Yu. A. Babanov, I. V. Golovshchikova, F. Boscherini, T.

Haubold, and S. Mobilio, *Physica B* **208&209**, 140 (1995).

⁵T. A. Grandi, V. H. F. dos Santos, and J. C. De Lima, *Solid State Commun.* **110**, 673 (1999).

⁶R. Birringer, H. Hahn, H. Höfler, J. Karch, and H. Gleiter, *Defect Diffus. Forum* **59**, 17 (1988).

⁷H. Gleiter, *Prog. Mater. Sci.* **33**, 223 (1989).

- ⁸J. C. De Lima, D. M. Trichês, V. H. F. dos Santos, and T. A. Grandi, *J. Alloys Compd.* **282**, 258 (1999).
- ⁹A. W. Weeber and H. Bakker, *Physica B* **115**, 93 (1988).
- ¹⁰D. K. Mukhopadhyay, C. Suryanarayana, and F. H. Froes, *Scr. Metall. Mater.* **30**, 133 (1994).
- ¹¹A. R. Yavari, P. J. Desré, and T. Benameur, *Phys. Rev. Lett.* **68**, 2235 (1992).
- ¹²E. Y. Gutmanas, in *Proceedings of the DGM Conference on New Materials by Mechanical Alloying Techniques*, edited by E. Arzt and L. Schultz (DGM Informationsgesellschaft, Oberursel, 1989), p. 129.
- ¹³H. J. Fecht, H. Hellstern, Z. Fu, and W. L. Johnson, *Advances in Powder Metallurgy* (Metal Powder Industries Federation, Princeton, NJ, 1989), Vols. 1–3, pp. 111–122.
- ¹⁴L. Schultz, *J. Less-Common Met.* **145**, 233 (1988).
- ¹⁵H. J. Fecht, *Acta Metall. Mater.* **38**, 1927 (1990).
- ¹⁶J. M. Smith and H. C. van Ness, *Introduction to Chemical Engineering Thermodynamics*, 3rd ed. (McGraw-Hill, Tokyo, 1975), p. 251.
- ¹⁷J. C. De Lima, E. C. Borba, C. Paduani, V. H. F. dos Santos, T. A. Grandi, H. R. Rechenberg, I. Denicoló, M. Elmassalami, and A. F. Barbosa, *J. Alloys Compd.* **234**, 43 (1996).
- ¹⁸C. Politis, *Physica B* **135**, 286 (1985).
- ¹⁹A. Corrias, G. Licheri, G. Vlaic, D. Raoux, and J. C. De Lima, in *European Conference on Progress in X-Ray Synchrotron Radiation Research*, 2nd ed., edited by A. Balerna, E. Bernieri and S. Mobilio (SIF, Bologna, 1990), Vol. 25, p. 689.
- ²⁰P. H. Shingu, K. N. Ishihara, K. Uenishi, J. Kuyama, B. Huang, and S. Nasu, in *Solid State Powder Processing, Minerals*, edited by A. H. Clauer and J. J. Barbadillo (Metals and Materials Society, Warrendale, PA, 1990), pp. 21–34.
- ²¹E. Gaffet, C. Louison, M. Harmelin, and F. Faudet, *Mater. Sci. Eng., A* **134**, 1380 (1991).
- ²²G. Veltl, B. Scholz, and H. D. Kunze, *Mater. Sci. Eng., A* **134**, 1410 (1991).
- ²³T. Fukunaga, M. Mori, K. Inou, and U. Mizutani, *Mater. Sci. Eng., A* **134**, 863 (1991).
- ²⁴A. O. Aning, Z. Wang, and T. H. Courtney, *Acta Metall. Mater.* **41**, 165 (1993).
- ²⁵H. P. Klug and L. E. Alexander, *X-Ray Diffraction Procedures*, 2nd, ed. (Wiley, New York, 1974), p. 656.
- ²⁶H. M. Rietveld, *J. Appl. Crystallogr.* **2**, 65 (1969).
- ²⁷TAPP, version 2.2, E. S. Microware, Inc., 2234 Wade Court, Hamilton, OH 45013.
- ²⁸Inorganic Crystal Structure Database, GMELIN-Institut für Anorganische Chemie and Fachinformationszentrum FIZ Karlsruhe, Germany.
- ²⁹G. F. Zhou and H. Bakker, *Phys. Rev. B* **48**, 13 383 (1993).